Electronic supplementary information

Influence of substituents on DNA and protein binding of cyclometalated Ir(III) complexes and anticancer activity

Sujay Mukhopadhyay[†], Roop Shikha Singh[†], Rajendra Prasad Paitandi[†], Gunjan Sharma[ξ], Biplob Koch[ξ], and Daya Shankar Pandey*†

[†]Departments of Chemistry, and [ξ]Zoology, Institute of Science, Banaras Hindu University, Varanasi – 221 005 (U.P.) India

Contents

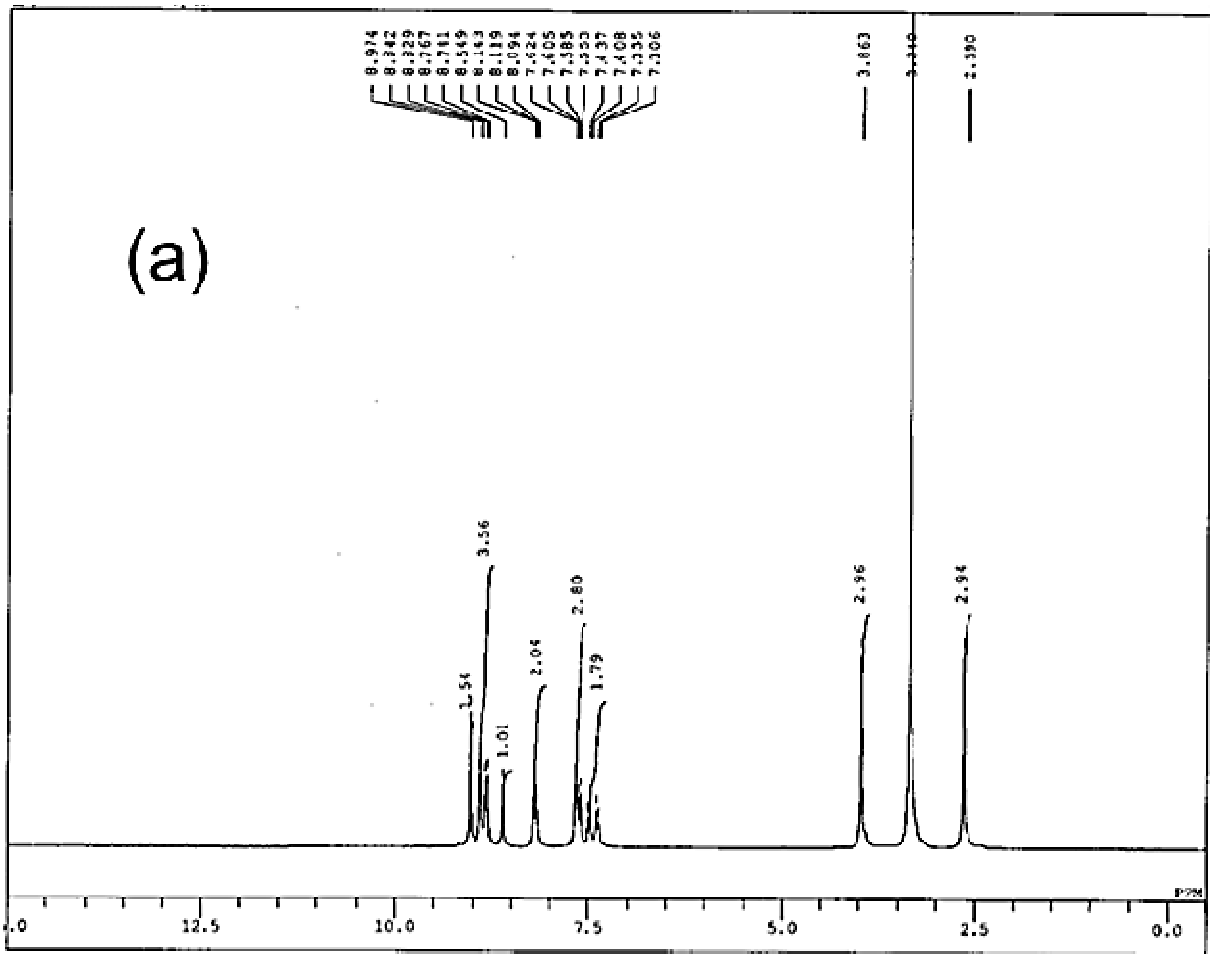
(a)
3.56
2.96
2.94
2.80
2.04
1.79
1.01
12.5
10.0
7.5
5.0
2.5
0.0

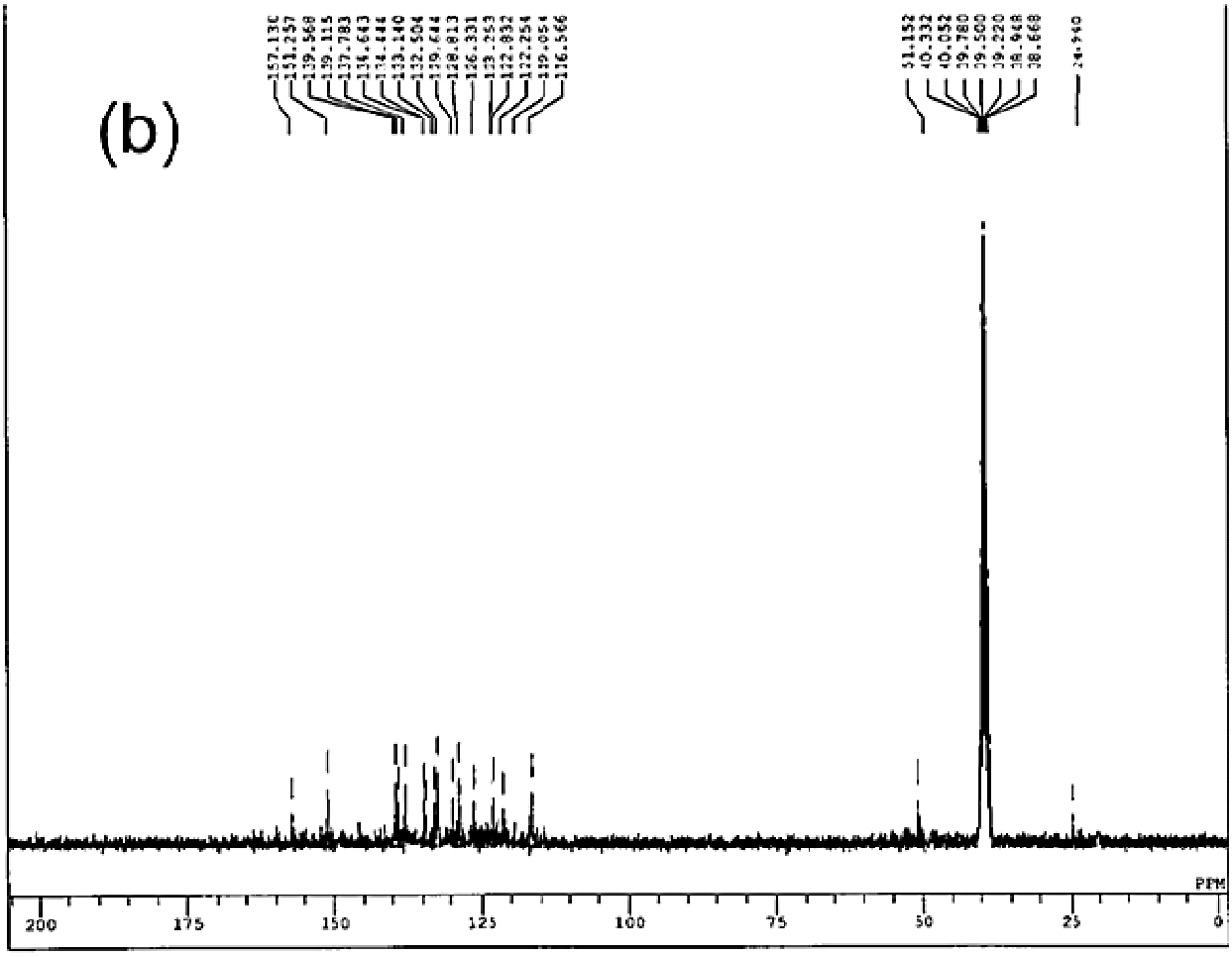

Figure S1: ^{1}H (a) and ^{13}C (b) NMR spectra of **L1**

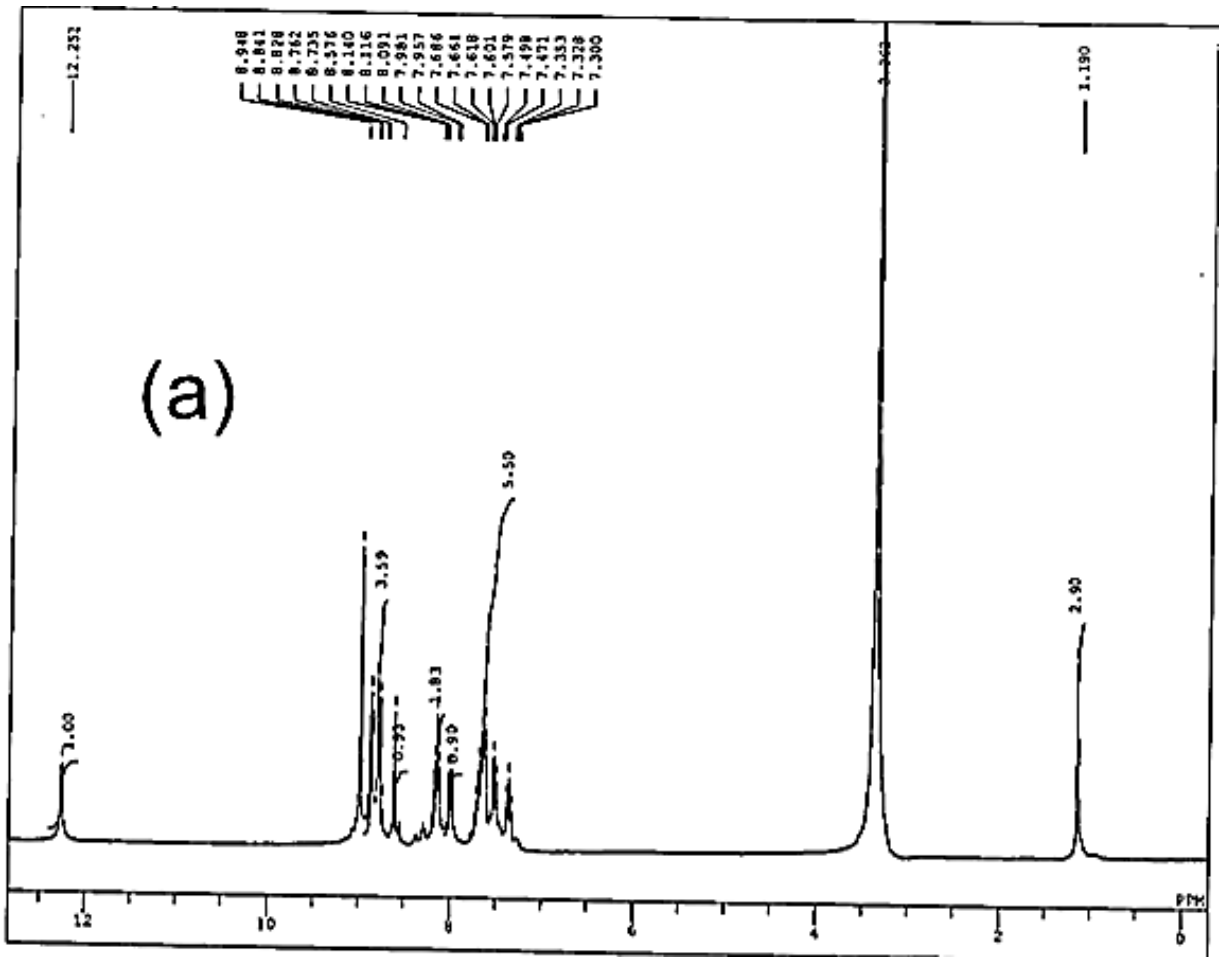
(a)
12.252
8.948
8.841
8.828
8.762
8.735
8.576
8.140
8.116
8.091
7.981
7.957
7.686
7.661
7.618
7.601
7.579
7.499
7.471
7.353
7.328
7.300
3.363
2.190
5.50
3.59
1.83
1.00
0.93
0.90
2.90
12
10
8
6
4
2
0
PPM

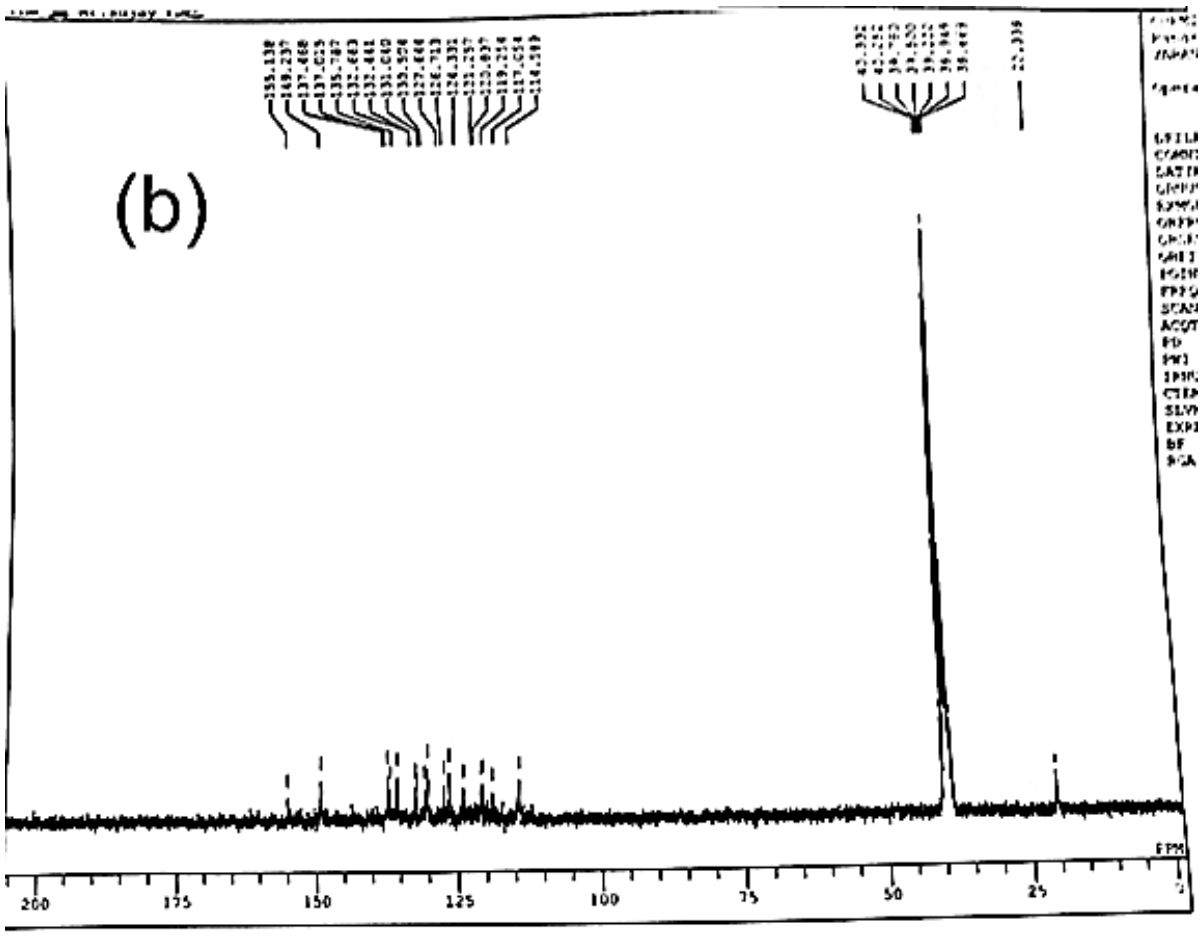

Figure S2: ^{1}H (a) and ^{13}C (b) NMR spectra of **L3**

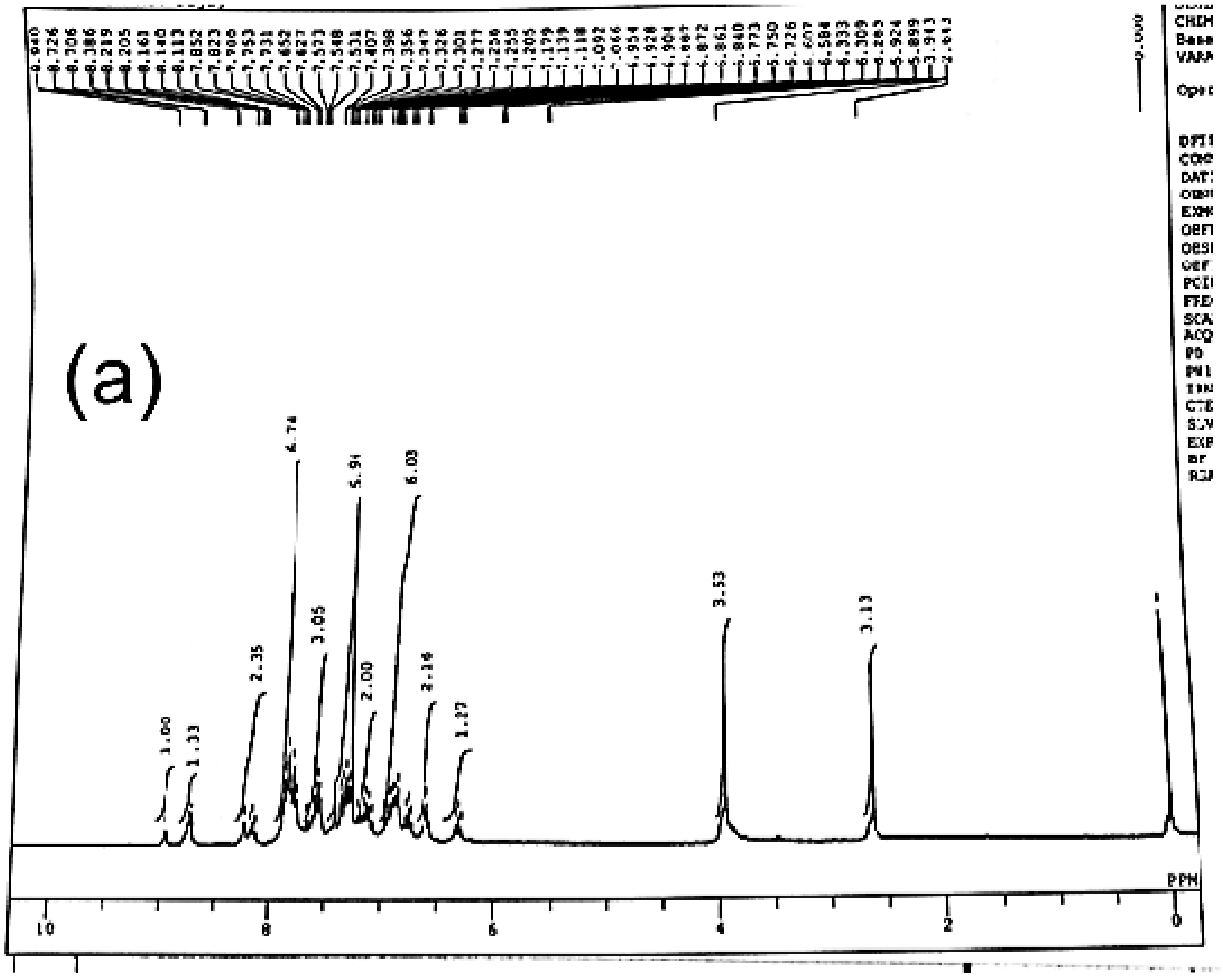
(a)
1.00
1.33
2.35
4.74
3.05
5.91
2.00
6.03
2.14
1.27
3.53
3.13
PPM
10
8
6
4
2
0

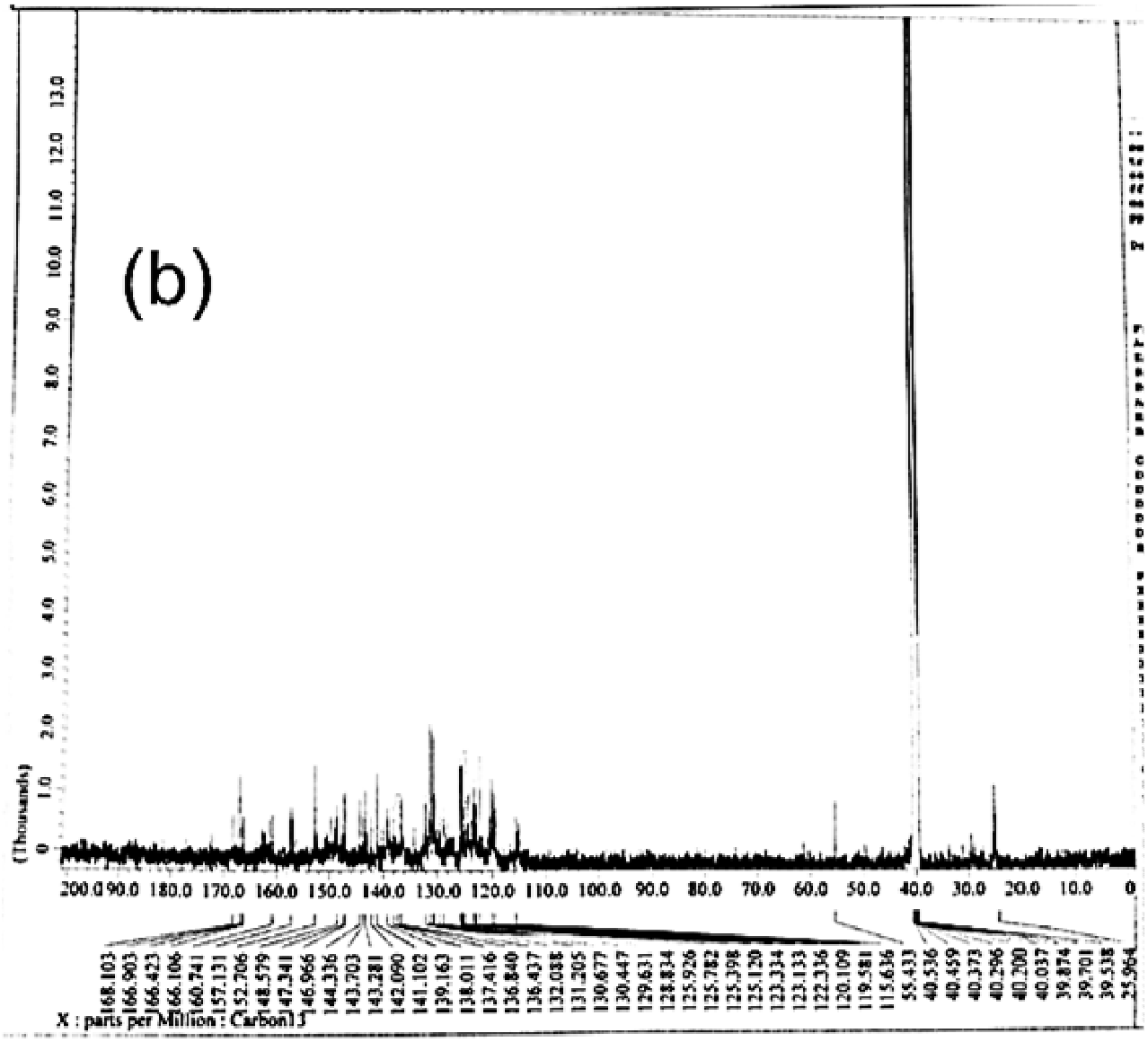

Figure S3: ^{1}H (a) and ^{13}C (b) NMR spectra of **1**

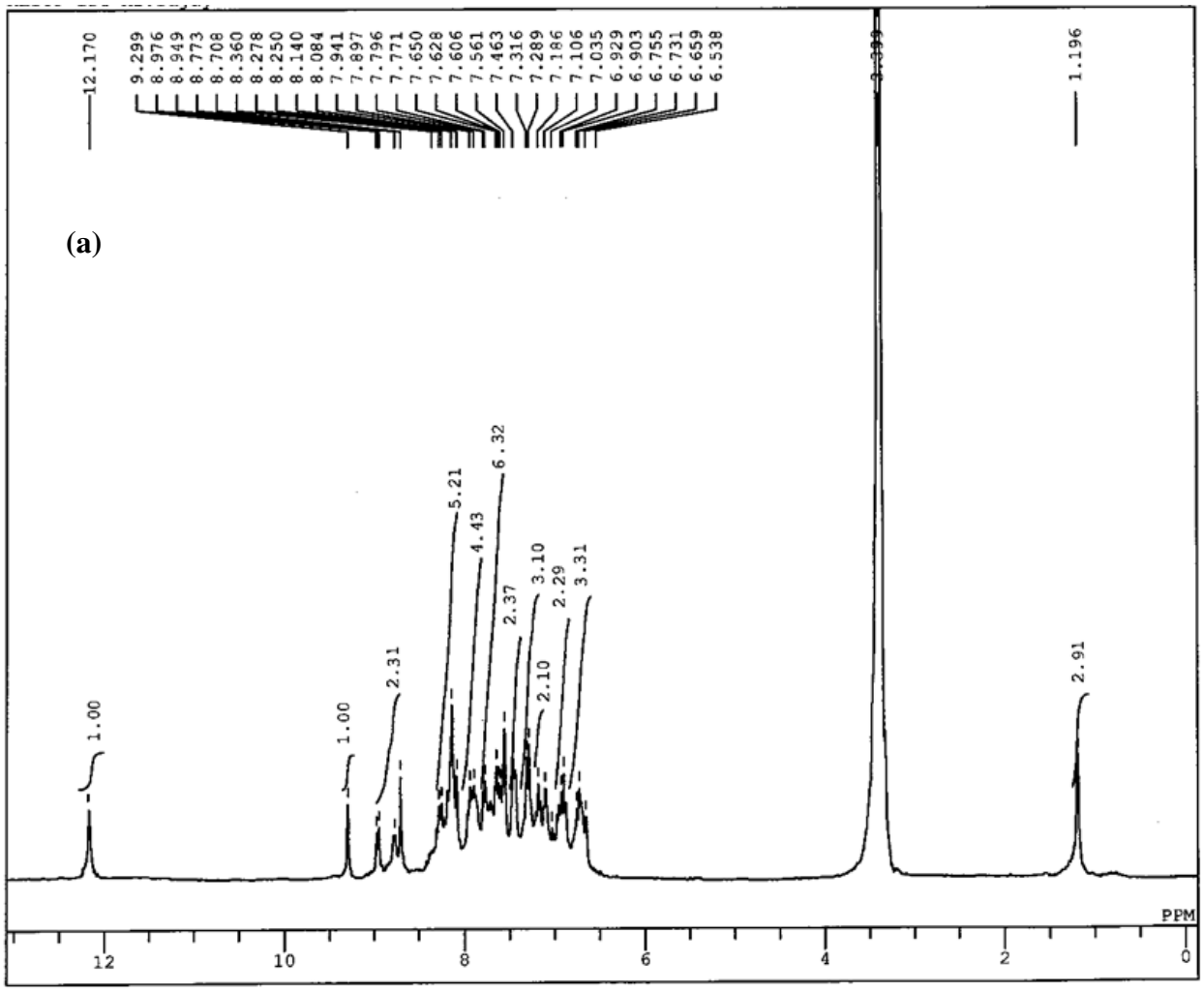
(a)
12.170
9.299
8.976
8.949
8.773
8.708
8.360
8.278
8.250
8.140
8.084
7.941
7.897
7.796
7.771
7.650
7.628
7.606
7.561
7.463
7.316
7.289
7.186
7.106
7.035
6.929
6.903
6.755
6.731
6.659
6.538
3.339
1.196
1.00
1.00
2.31
5.21
4.43
6.32
2.37
3.10
2.29
3.31
2.10
2.91
PPM
12
10
8
6
4
2
0

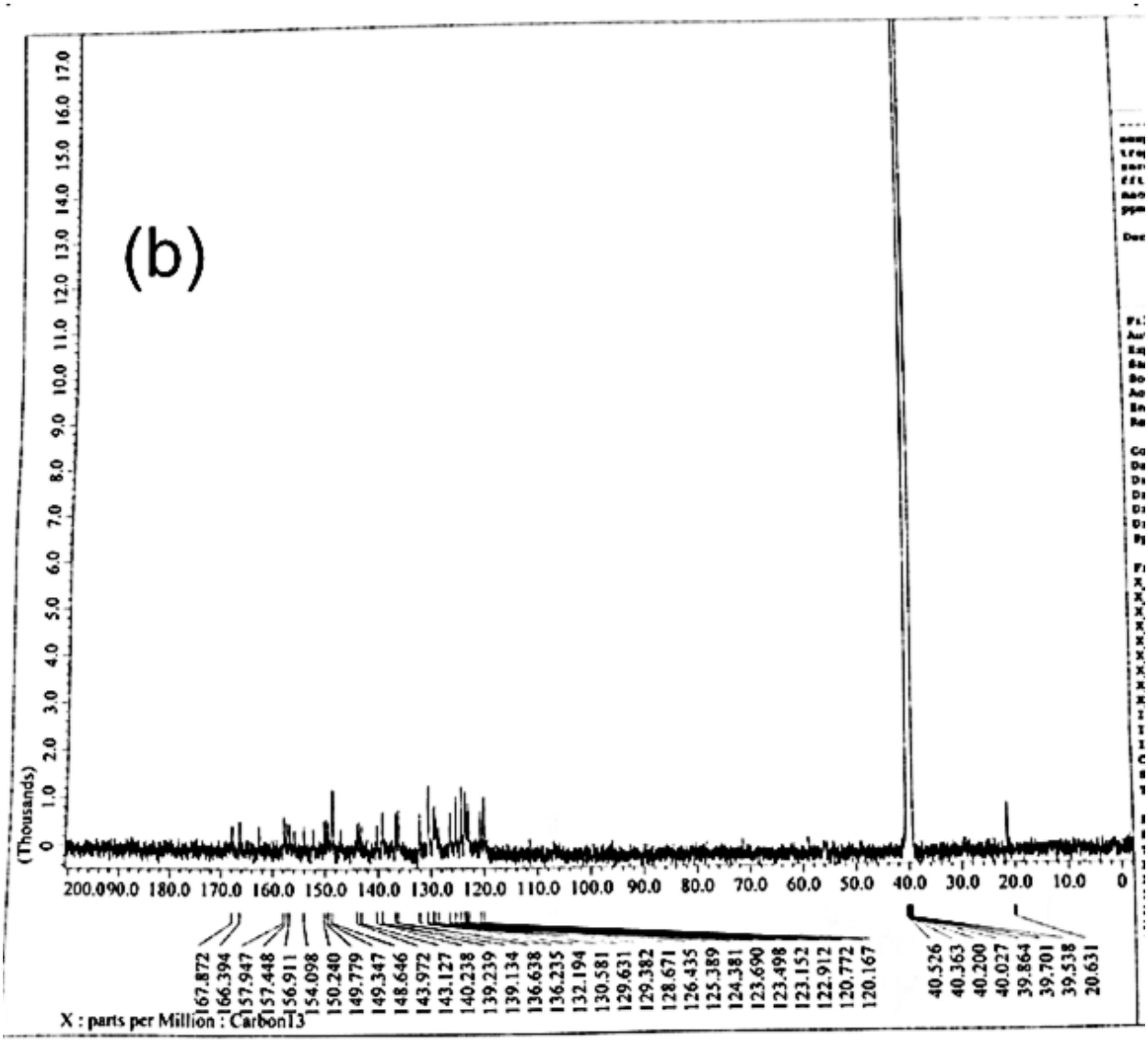

Figure S4: ^{1}H (a) and ^{13}C (b) NMR spectra of **3**

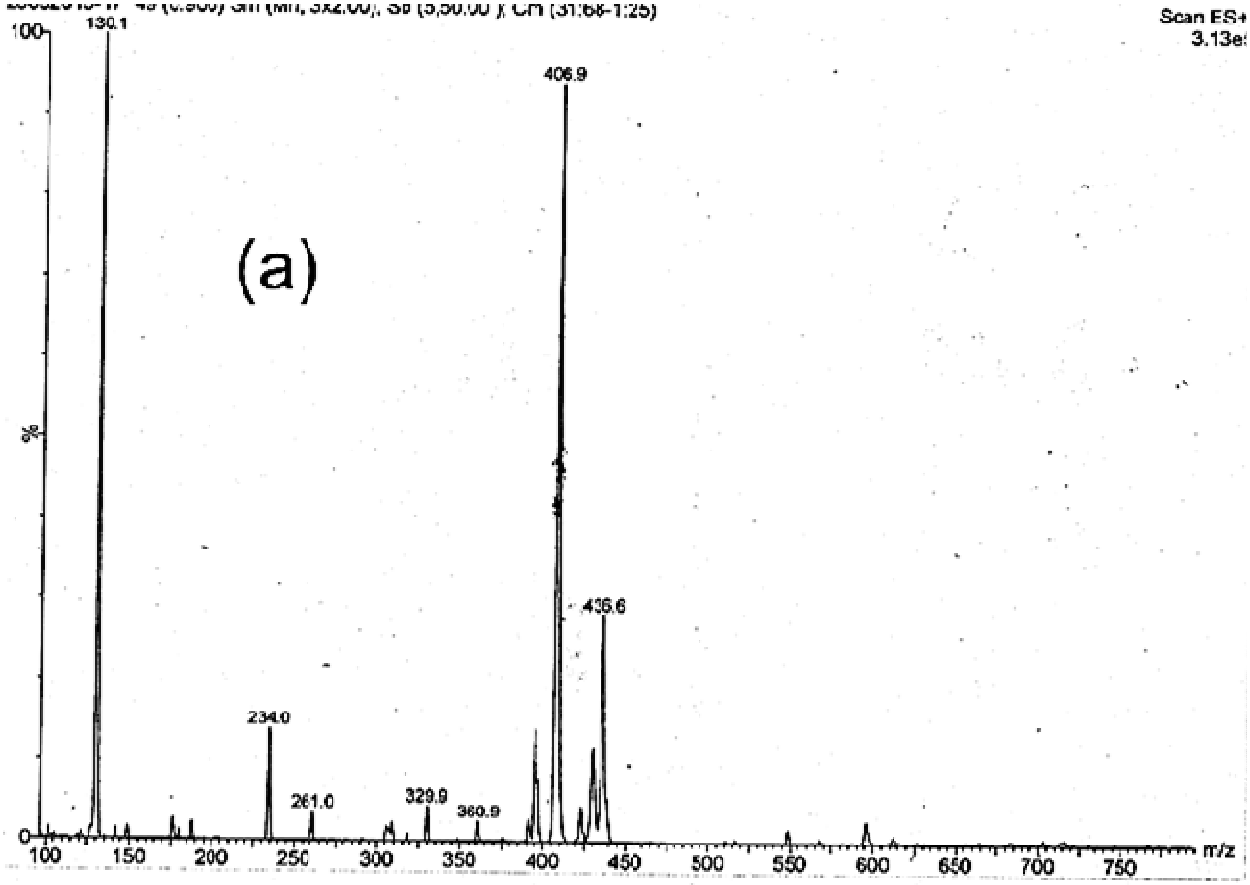
Scan ES+
3.13e
100
%
0
130.1
406.9
436.6
234.0
261.0
329.9
360.9
(a)
100
150
200
250
300
350
400
450
500
550
600
650
700
750
m/z

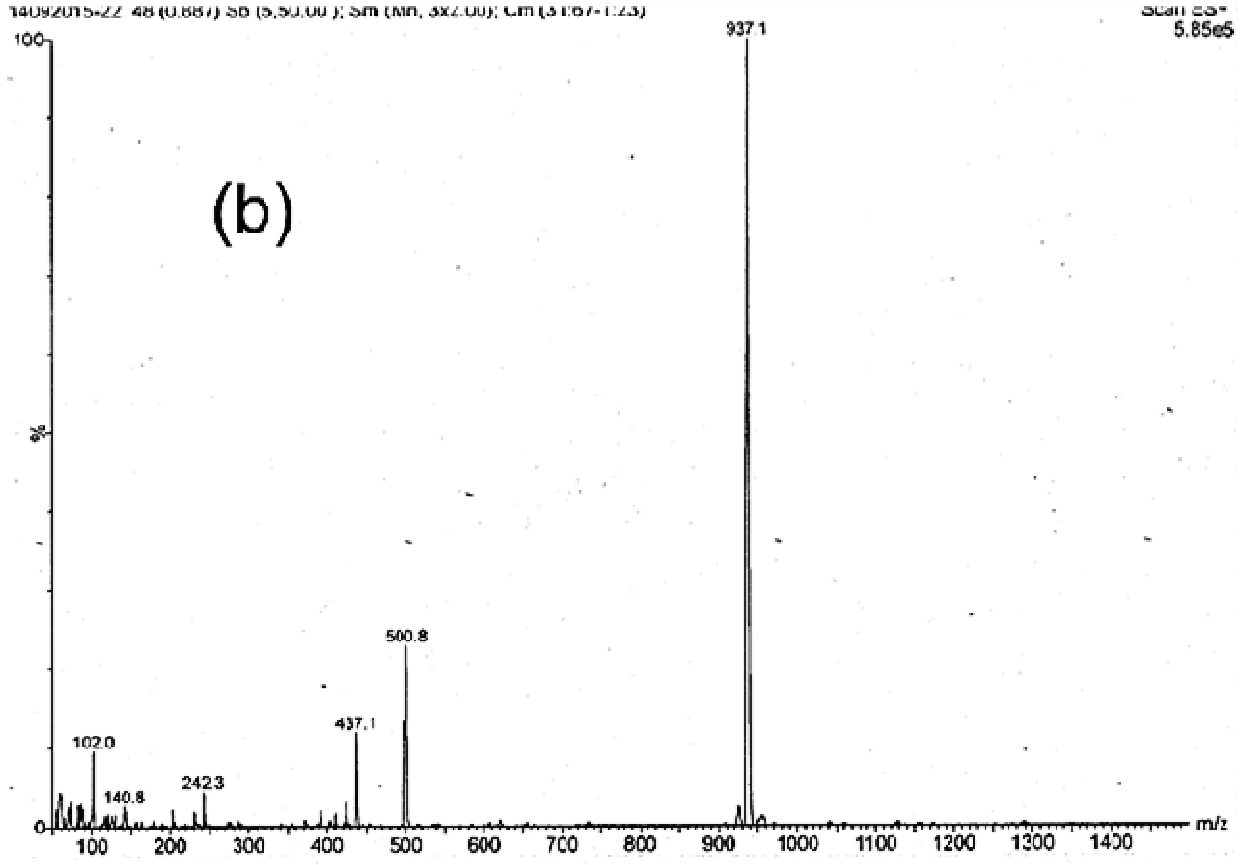

Figure S5: ESI-MS spectra of **L1** (a) and **1** (b)

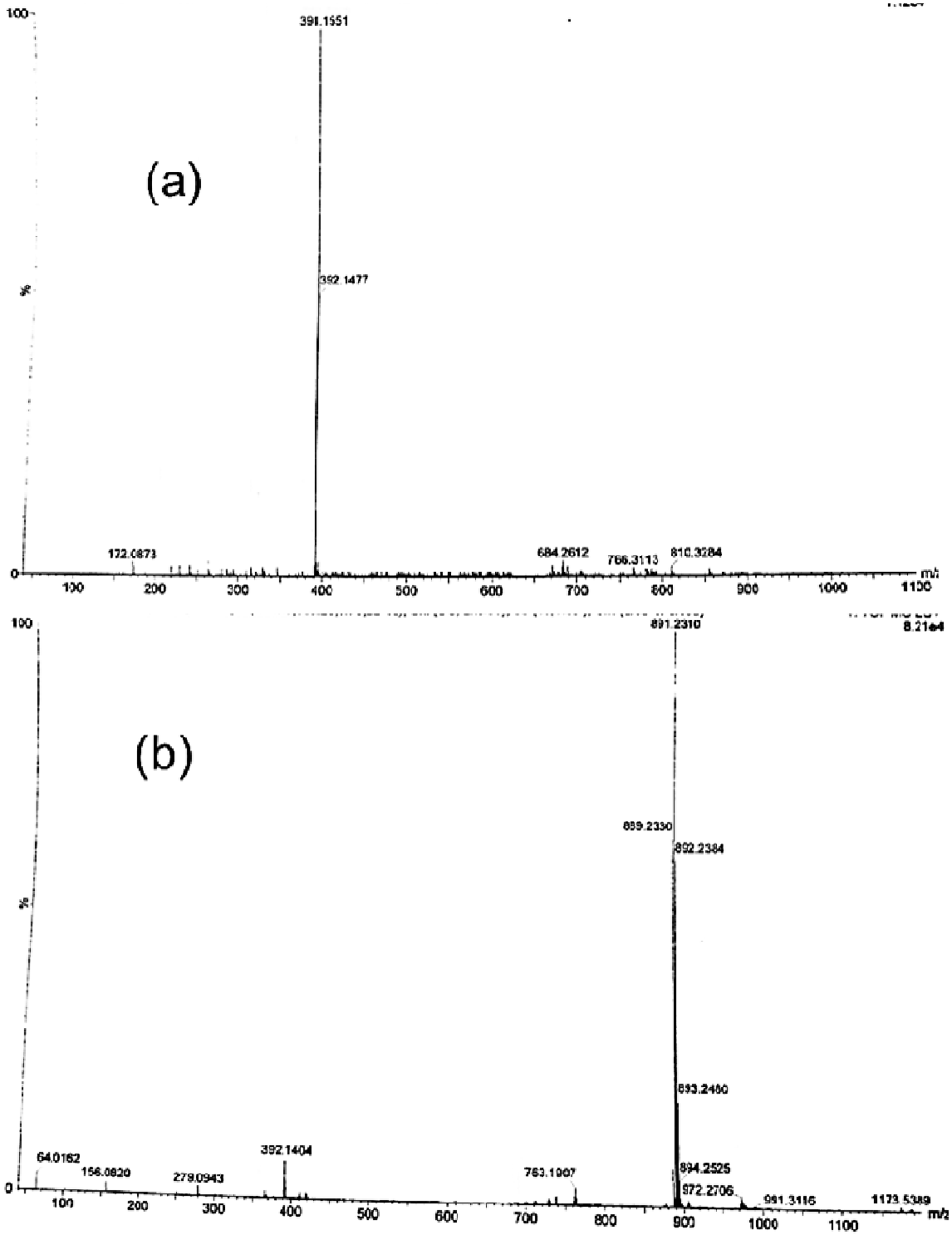

Figure S6: ESI-MS spectra of **L3** (a) and **3** (b)

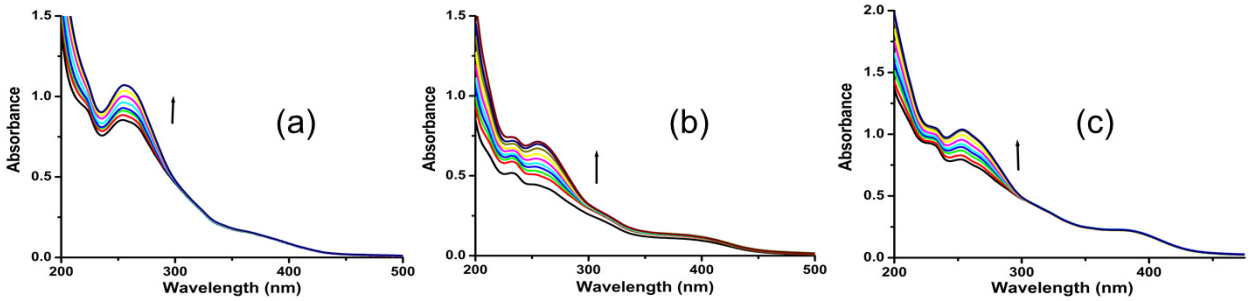

Figure S7: UV/vis spectra of **1** (a) **2** (b) and **3** (c) in EtOH : PBS (1:1) with an increasing concentration of CT DNA (0–20 μM) at rt. Arrow shows absorbance increases upon increasing CT DNA concentration.

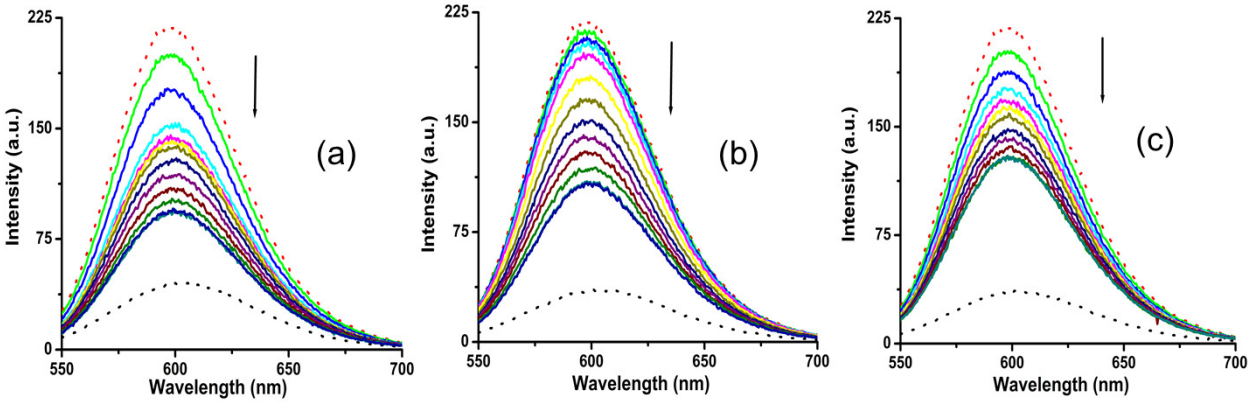

Figure S8: Fluorescence spectra of EB (black dotted) bound to CT DNA (red dotted) and in presence of (a) **1**, (b) **2**, (c) **3**. [EB, 10 μM; DNA, 10 μM, [**1**]–[**3**] 0–50 μM]. Arrow shows decrease in emission intensity upon increasing the amounts of **1**–**3**.

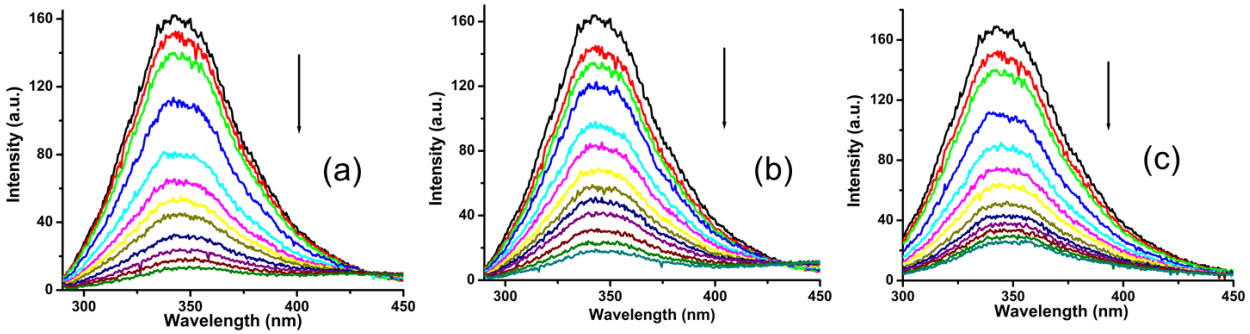

Figure S9: Emission spectrum of BSA (0.5 μM; λ_{ex}, 280 nm; λ_{em}, 343 nm) in presence of increasing amounts of (a) **1**, (b) **2**, and (c) **3** (0–50 μM).

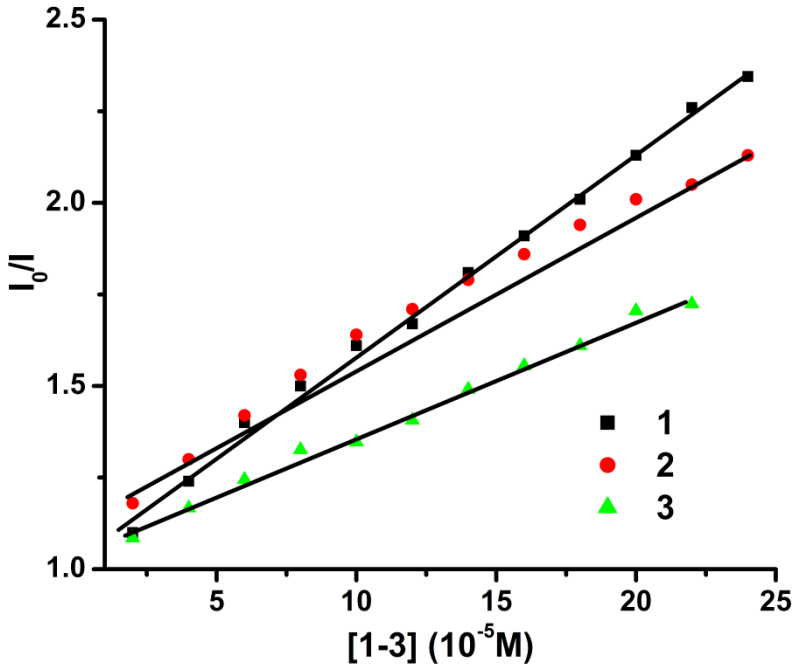

Figure S10: Stern-Volmer plots of the EB-DNA fluorescence titration for complexes **1–3**

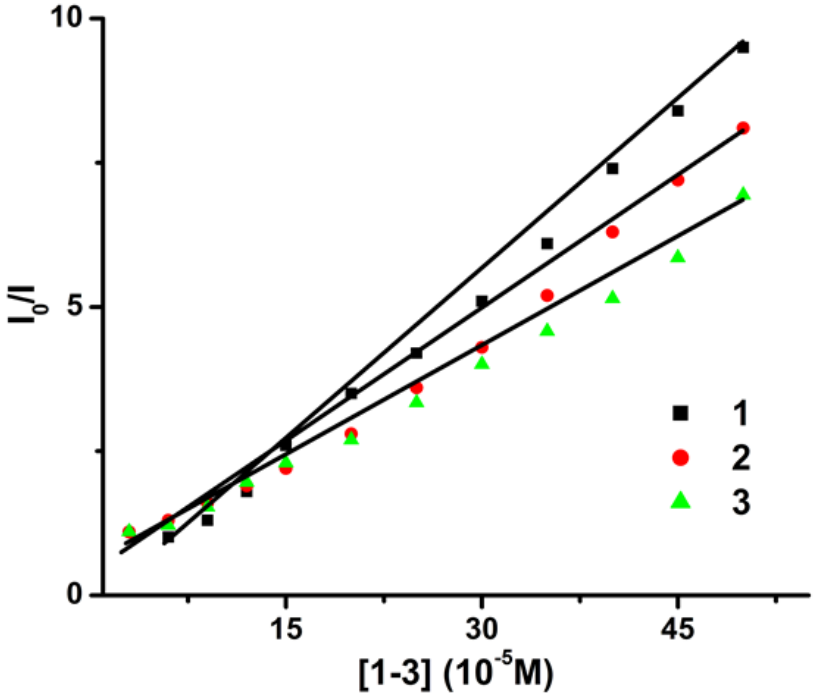

Figure S11: Stern-Volmer plots of the BSA fluorescence titrations of **1–3**.

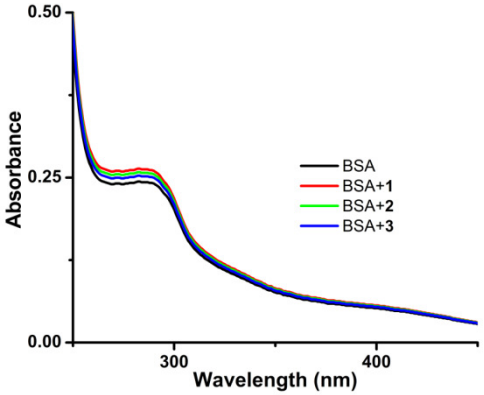

Figure S12. UV–vis absorption spectra of BSA (tris-HCl buffer, c, 10 μM, pH ~7.5) in presence of **1**–**3** (c, 5 μM).

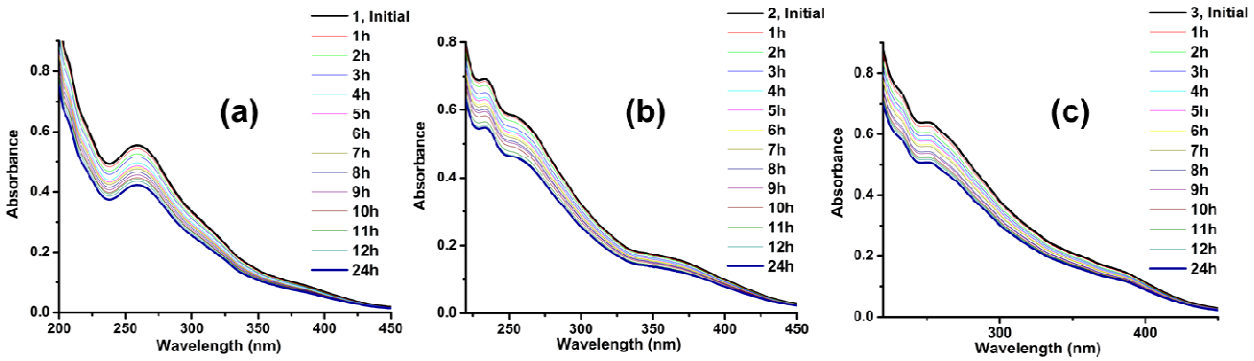

Figure S13. UV-vis absorption spectra of **1**-**3** in water from 1-24 h.

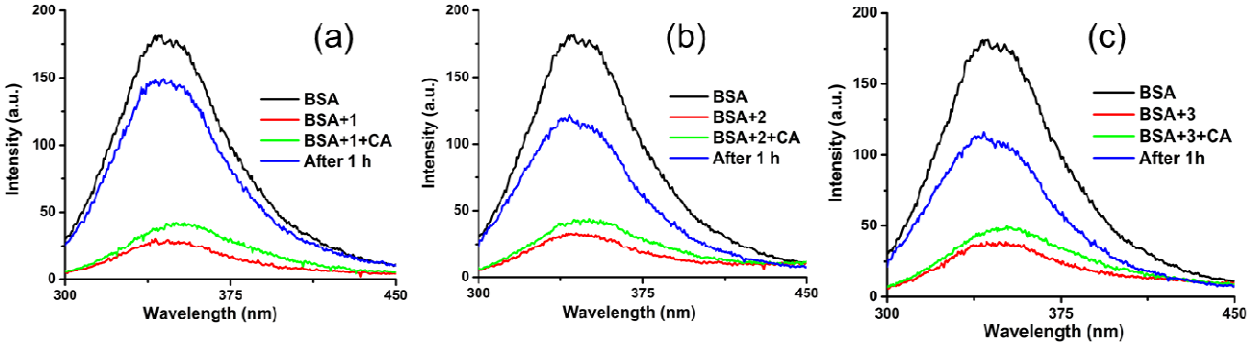

Figure S14. Fluorescence spectral changes upon addition of **1**, (a); **2**, (b); **3** (c) in BSA solution and after addition of citric acid (CA).

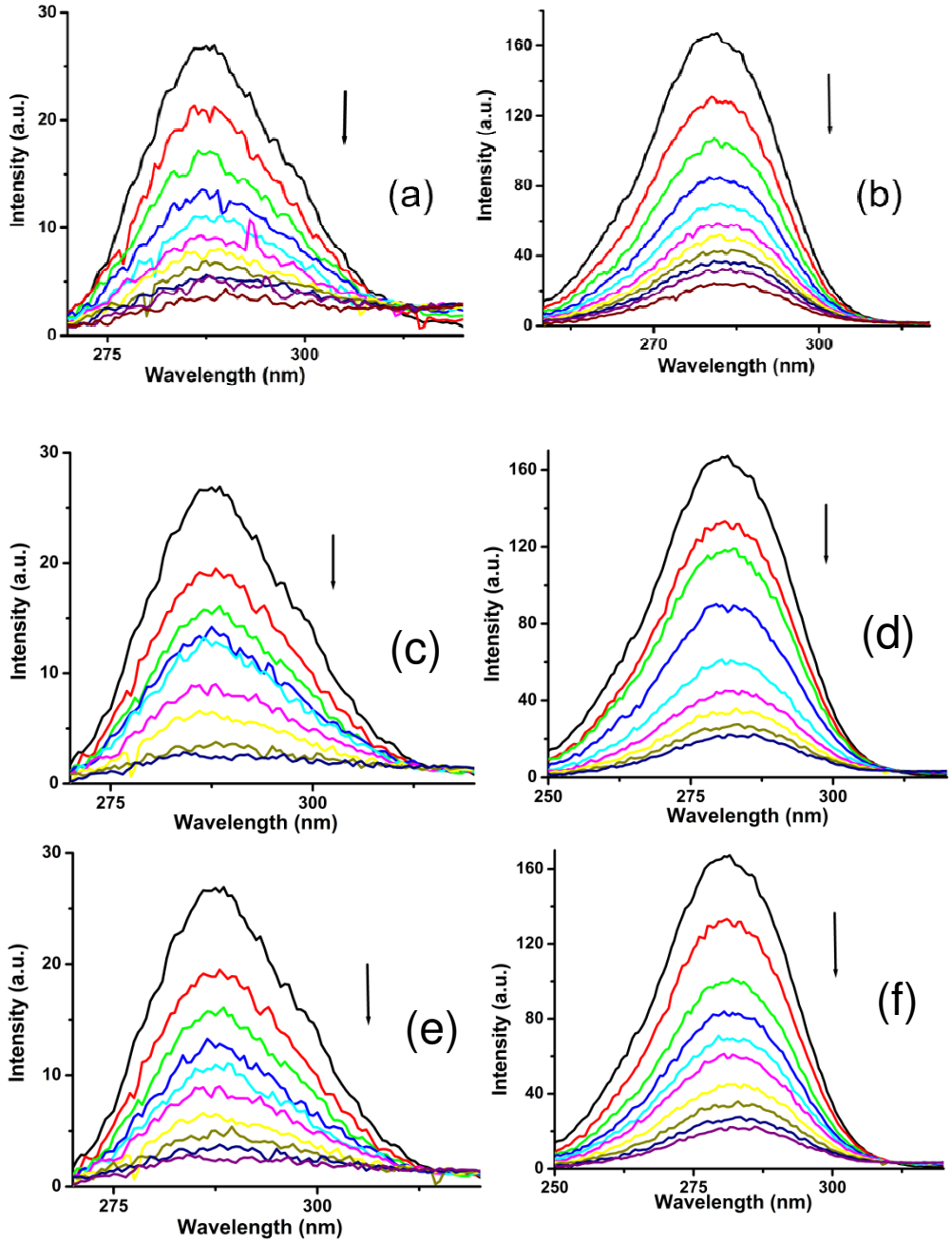

Figure S15: Synchronous spectra of BSA (0.5 μM) in presence of increasing amounts of the complexes **1** (a), **2** (c) and **3** (e) (0–50 μM) in the wavelength difference of $\Delta\lambda$ = 15 nm. Synchronous spectra of BSA in presence of increasing amounts of complexes **1** (b), **2** (d) and **3** (f) in the wavelength difference of $\Delta\lambda$ = 60 nm. Arrows show emission intensity decrease upon increasing the concentration of complexes.

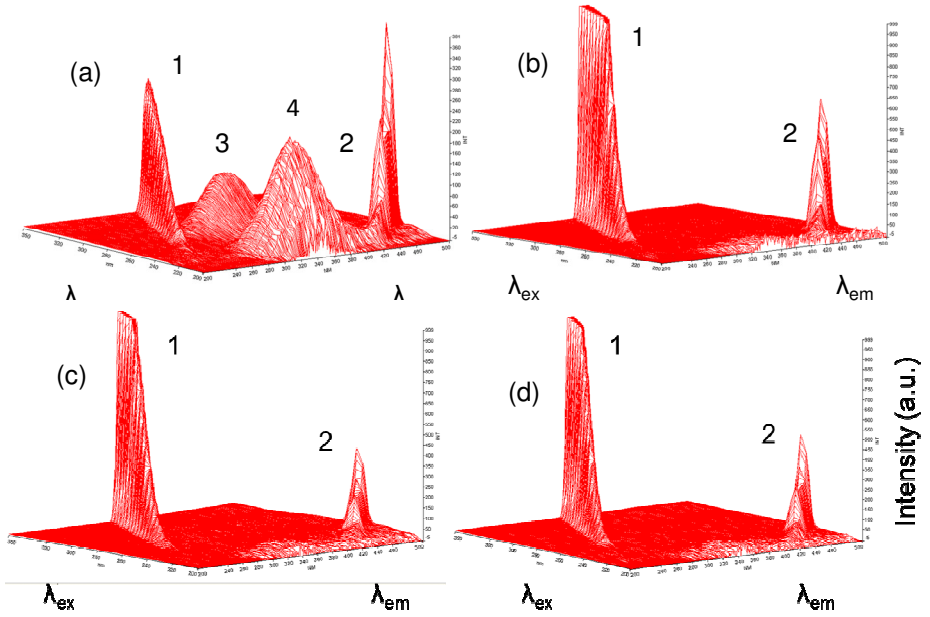

Figure S16: 3D fluorescence spectra of BSA (a), BSA + **1** (b), BSA + **2** (c) BSA + **3** (d); [BSA] = 10^{-6} molL^{-1}, [**1**, **2**, **3**] = 10^{-5} molL^{-1}.

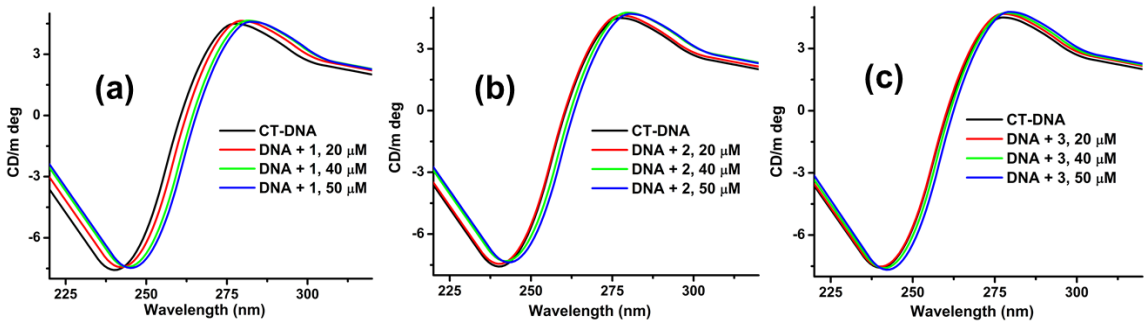

Figure S17: CD-spectra of CT-DNA in the absence and presence of the complexes **1**–**3**, [DNA] = 100 μM, [complex] = 0-50 μM.

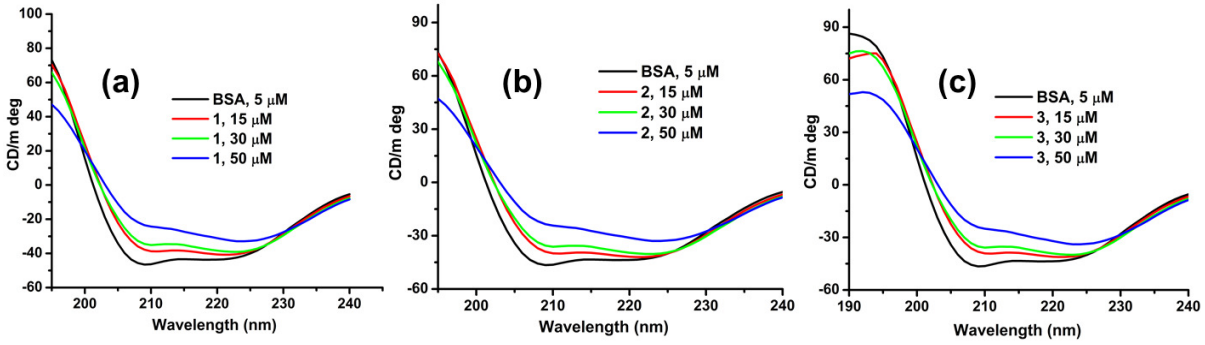

Figure S18: CD spectra of BSA with (a) **1** and (b) **2** and **3** (c), [BSA] = 5 μM, [complexes] = 0-50 μM, pH = 7.4.

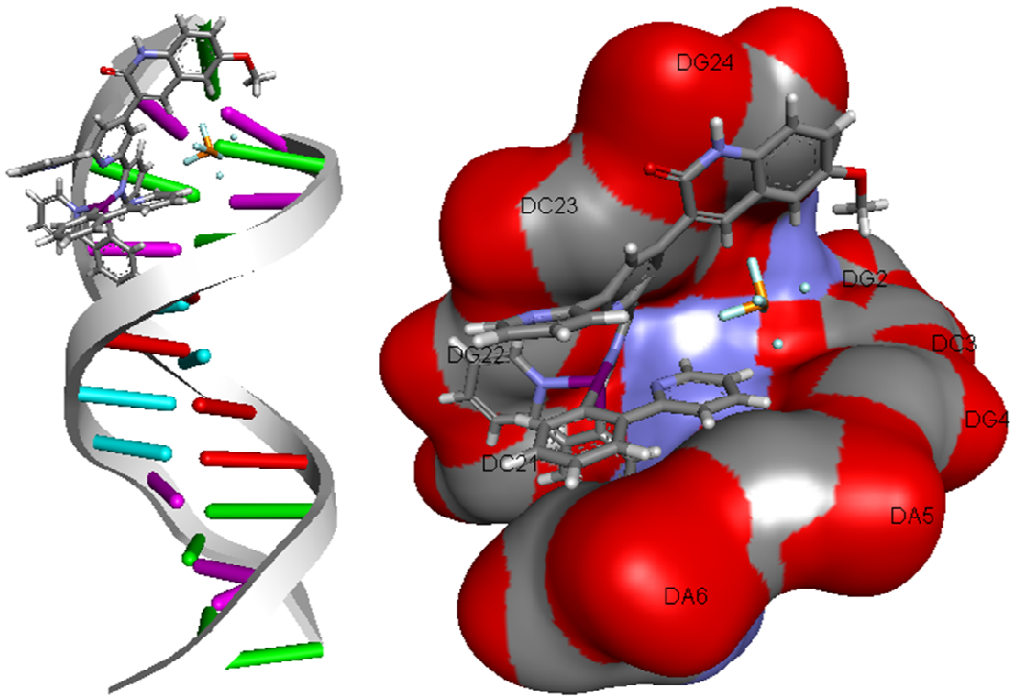

Figure S19: Molecular docked model of **2** with DNA (PDB ID: 1BNA).

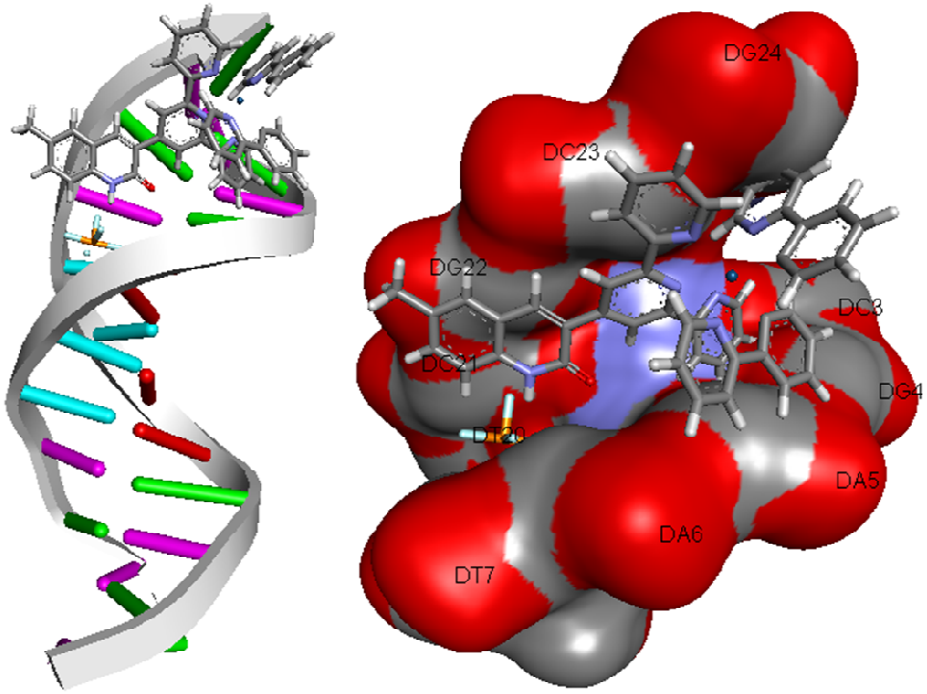

Figure S20: Molecular docked model of **3** with DNA (PDB ID: 1BNA).

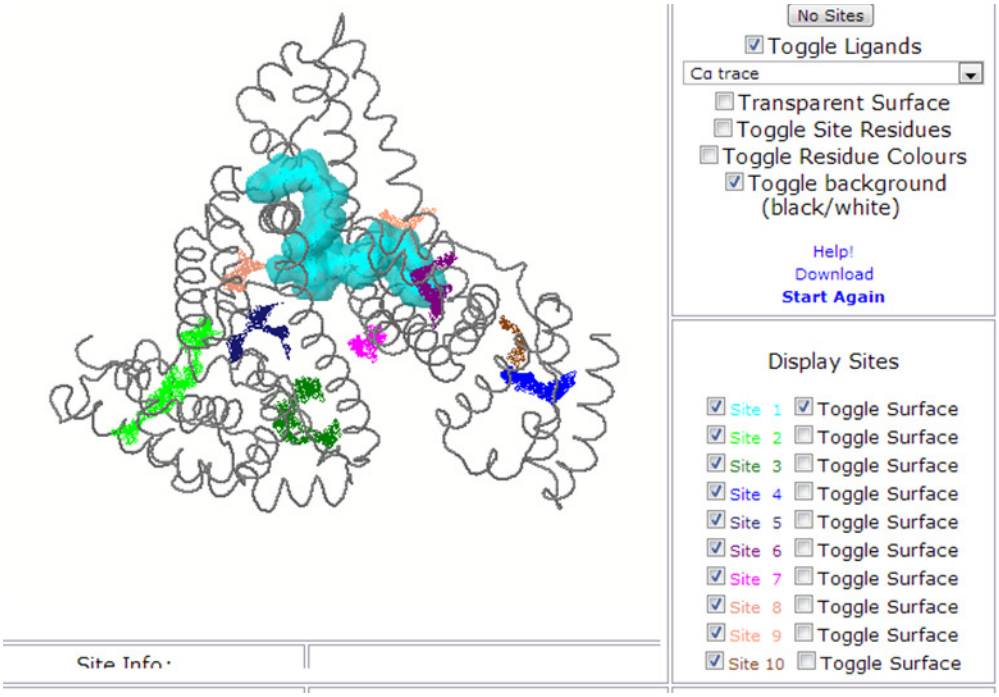

Figure S21: Most probable 10 (ten) binding sites of HSA (PDBID: 1h9z).

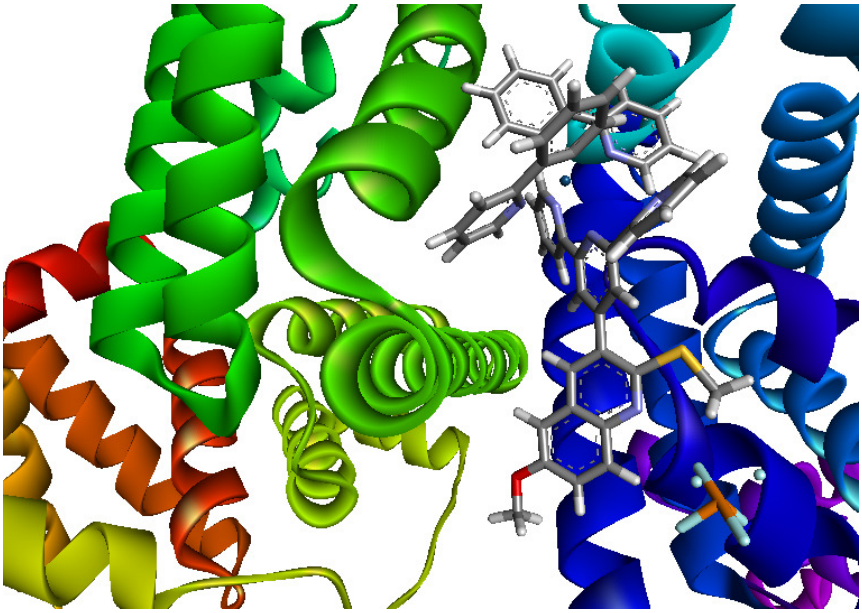

Figure S22. Zoomed Docked model of **1** located within the hydrophobic pocket of HSA.

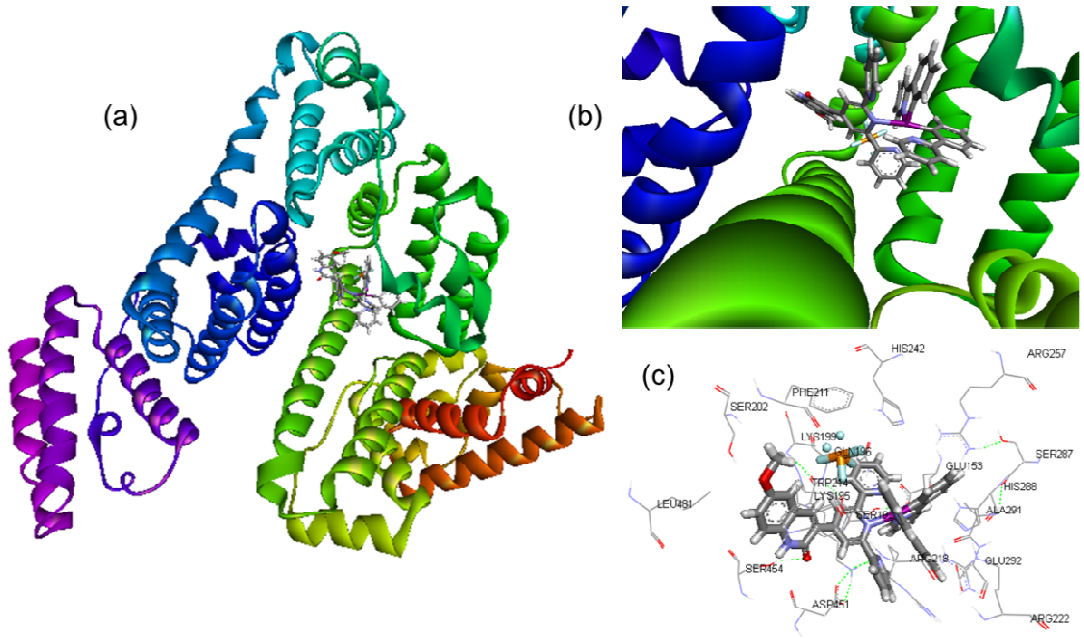

Figure S23. (a) Molecular docked model of **2** located within the hydrophobic pocket of HSA (PDB ID: 1h9z); (b) zoomed interaction mode between **2** (stick) and HSA (cartoon); (c) the interaction mode between **2** and polypeptide units.

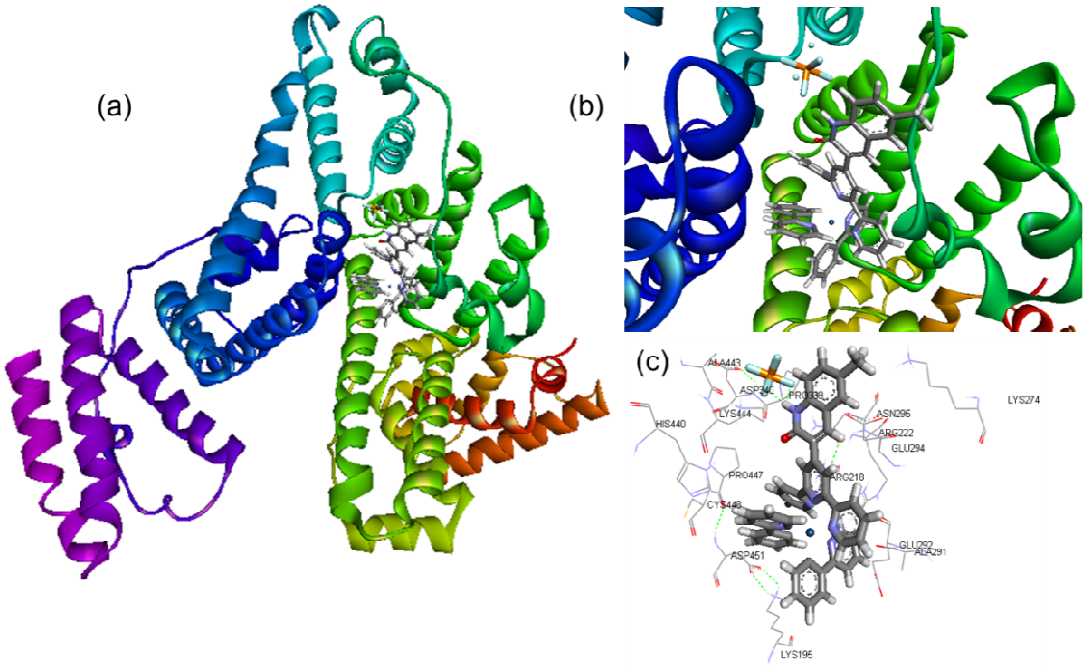

Figure S24. (a) Molecular docked model of **3** located within the hydrophobic pocket of HSA (PDB ID: 1h9z); (b) zoomed interaction mode between **3** (stick) and HSA (cartoon); (c) the interaction mode between **3** and polypeptide units.

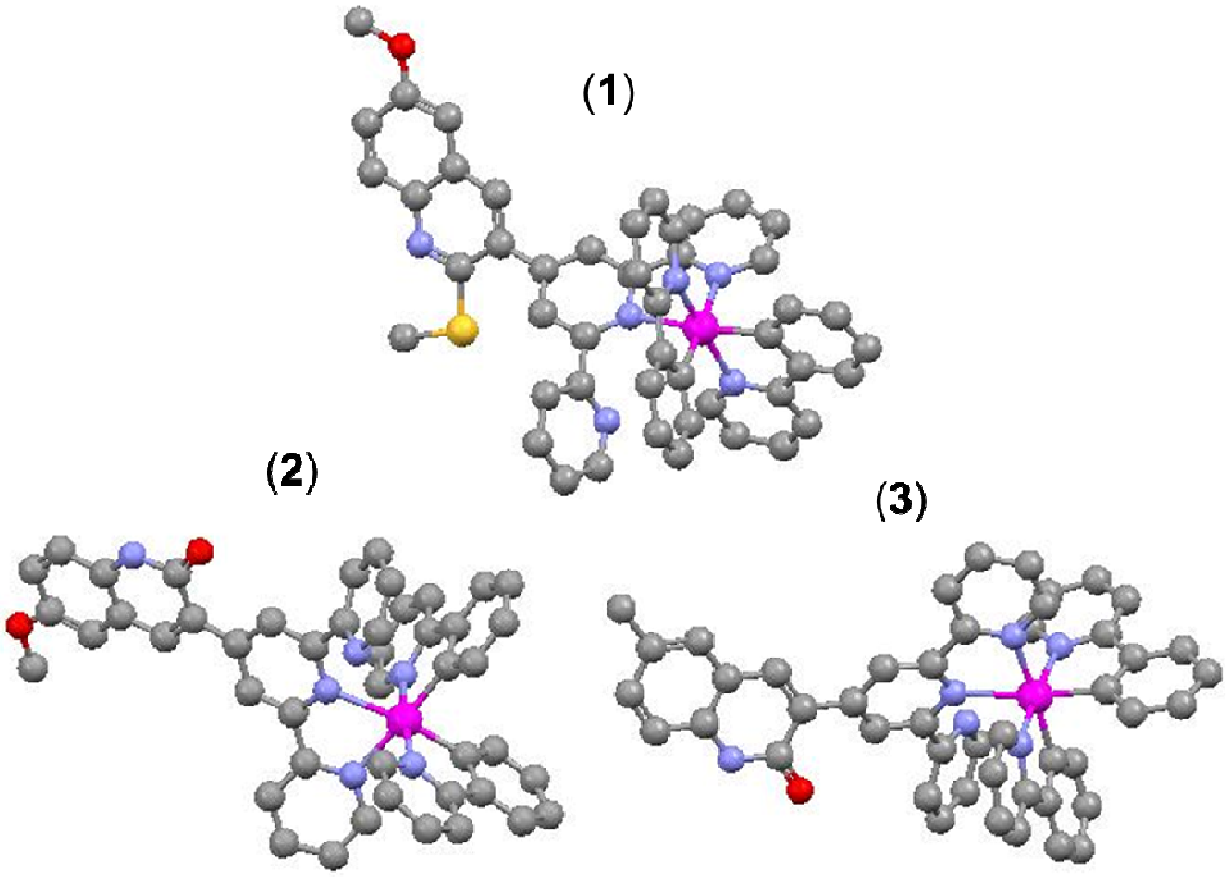

Figure S25. DFT optimized structures of **1 – 3**, H- atoms and PF_6^- are omitted for clarity.

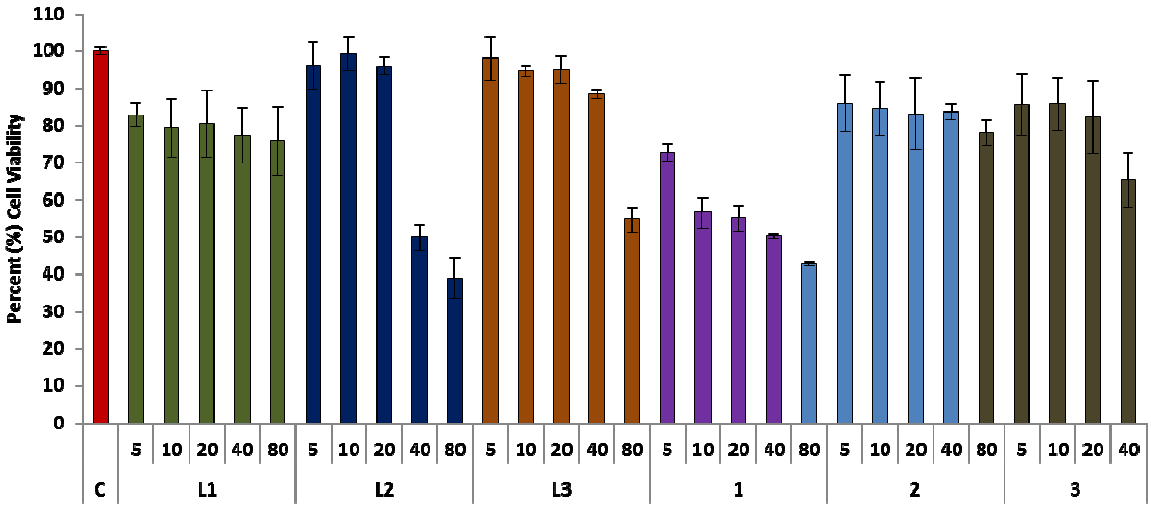

Figure S26. Percent cell viability and antiproliferation profile of ligands (**L1**-**L3**) and their complexes (**1**-**3**) against human breast cancer (MDA-MB-231) cells after 24 h of exposure.

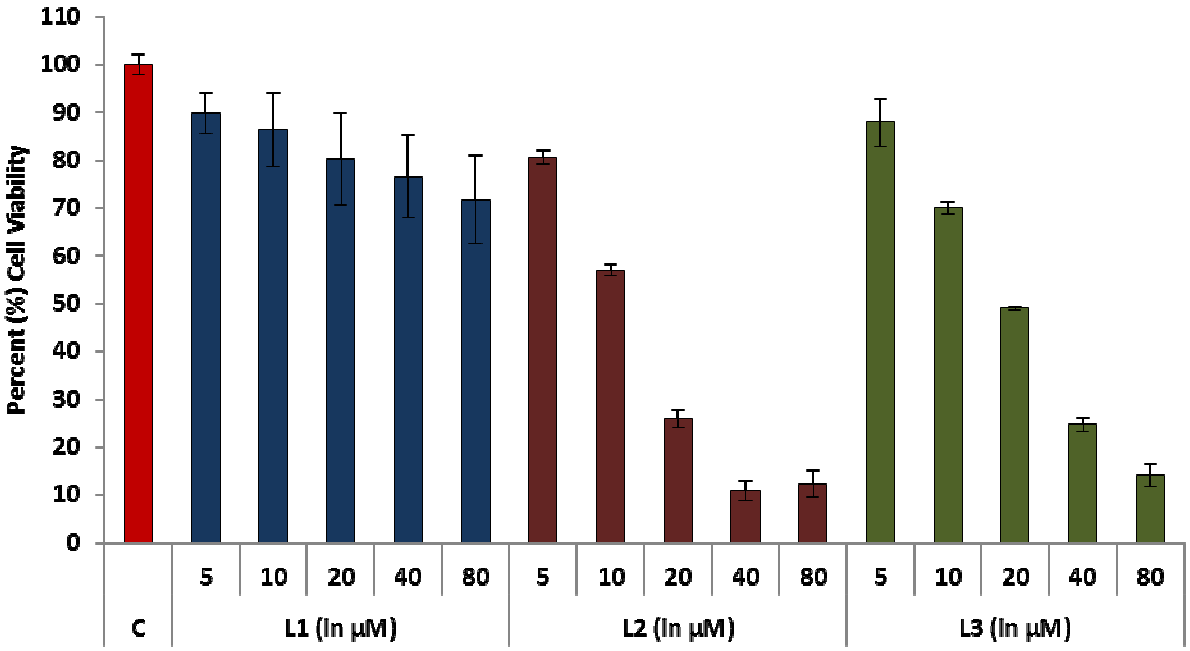

Figure S27. Percent cell viability and antiproliferation profile of ligands (**L1**-**L3**) against HeLa cell line after 24 h of exposure.

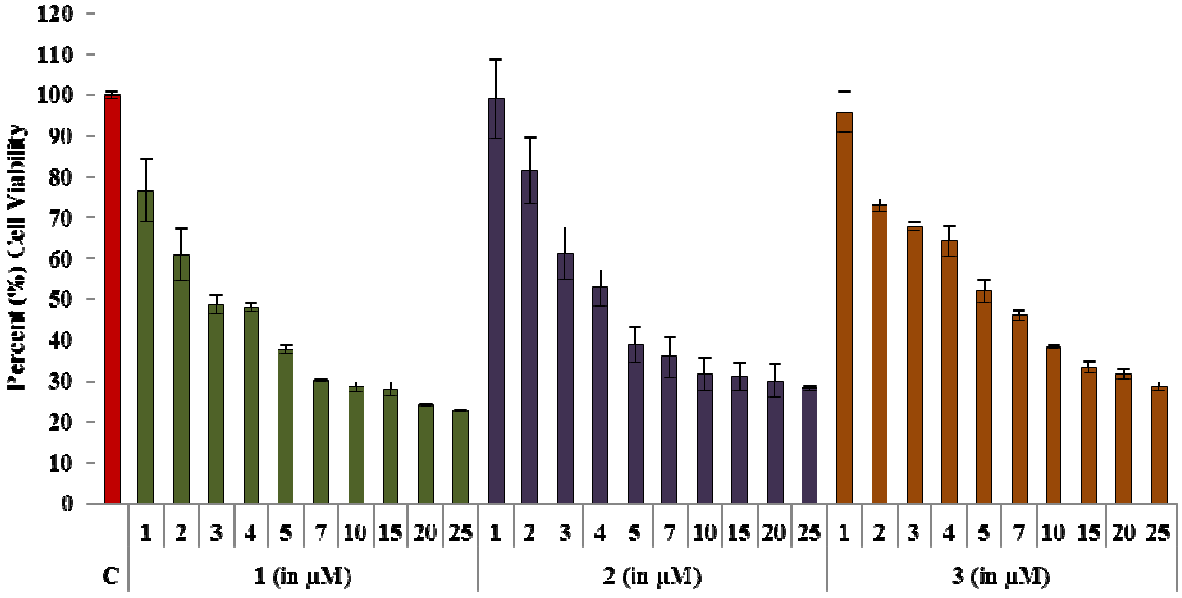

Figure S28. Percentage cell viability and antiproliferation profile of **1**-**3** against HeLa cells after 24 h of exposure.

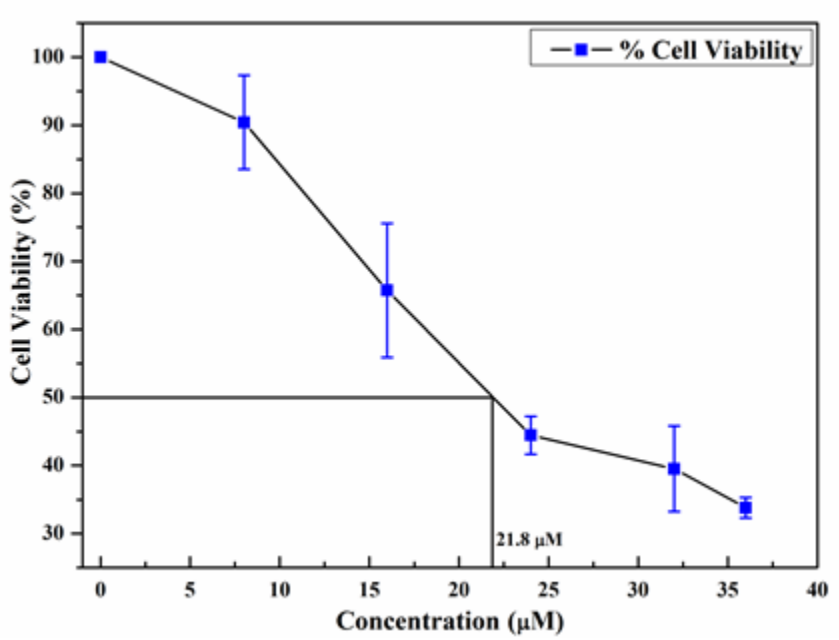

Figure S29. Percentage cell viability and antiproliferation profile of cisplatin against HeLa cells after 24 h of exposure.

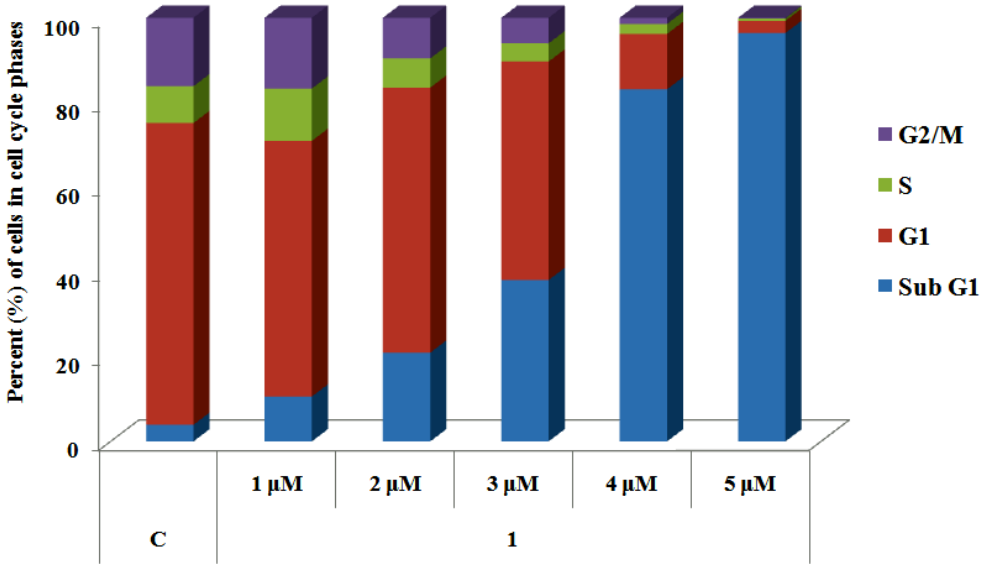

Figure S30: Histogram shows percentage of cells in different cell cycle phases.

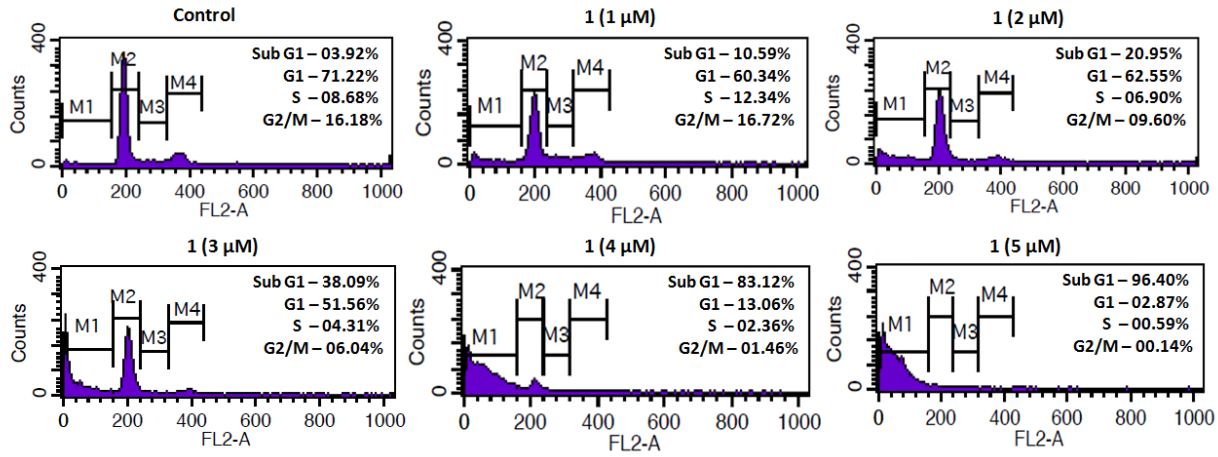

Figure S31: Flow cytometric analysis of control and treated HeLa cells with different concentrations of **1**.

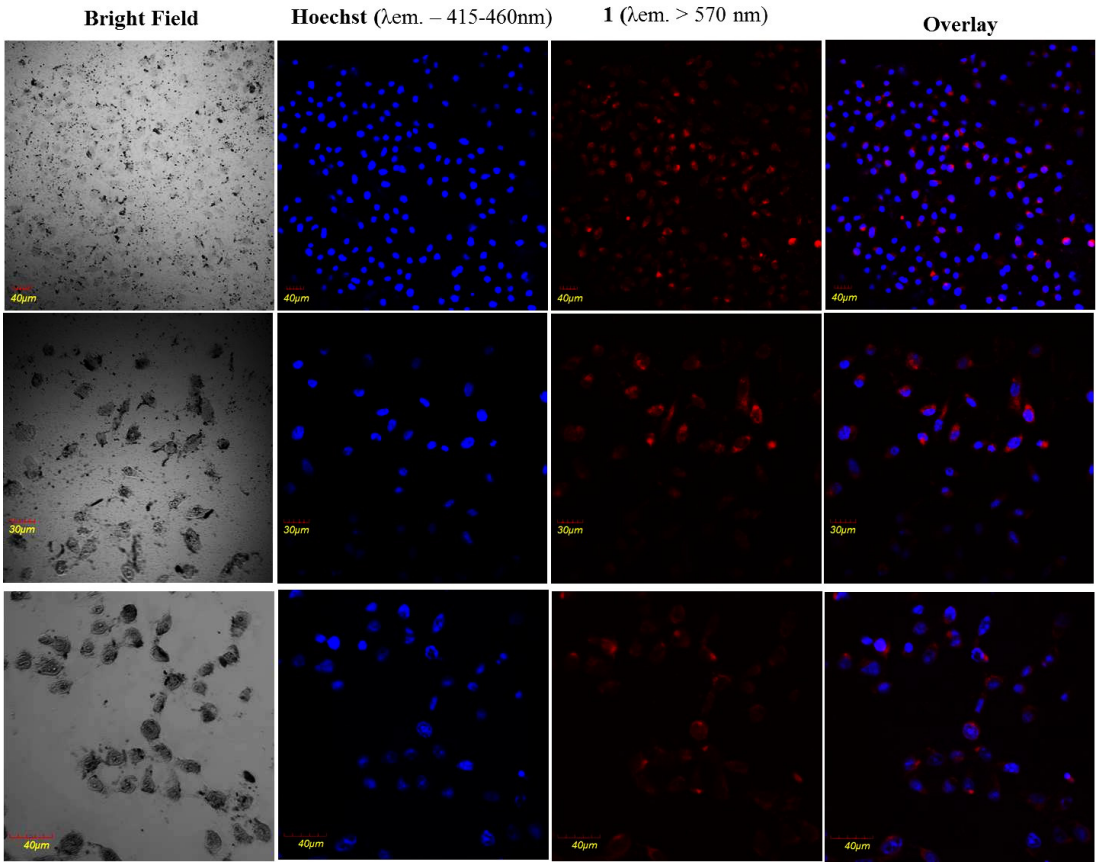

Figure S32: Confocal microscopic images of HeLa cells treated with dual staining of Hoechst and complex **1**.

Table S1. Crystal data and structure refinement parameters for **3**.

Crystal parameters	**3**
Empirical formula	$C_{47}H_{34}F_6IrN_6OP$
Formula weight	1035.99
Crystal system	Monoclinic
Space group	*P 21/c*
a (Å)	14.8319 (12)
b (Å)	8.4490 (8)
c (Å)	35.5020 (4)
α (deg)	90.000
β (deg)	99.459 (3)
γ (deg)	90.000
V ($Å^3$)	4388.4 (7)
Color and habit	Red, Block
Z	4
dcal (g/cm^3)	1.562
Temperature (K)	296 (2)
wavelength (Å)	0.71073
μ (mm^{-1})	3.147
GOF on F^2	1.048
R indices (All data)	R_1 = 0.1253 wR_2 = 0.2156
final R indices [I > 2σ(I)]	R_1 = 0.0750 wR_2 = 0.1966

Table S2. Selected bond lengths and bond angles of **3**.

3	**Bond lengths (Å)**	**3**	**Bond Angles (˚)**
Ir–C7	2.00 (9)	C7–Ir–C27	88.5 (4)
Ir–C27	2.01 (8)	C7–Ir–N3	93.3 (4)
Ir–N3	2.03 (9)	C27–Ir–N3	81.1 (4)
Ir–N1	2.04 (9)	C7–Ir–N1	81.2 (4)
Ir–N2	2.14 (7)	C27–Ir–N1	94.3 (4)
Ir–N4	2.27 (8)	N3–Ir–N1	172.9 (3)
		C7–Ir–N2	93.4 (3)
		C27–Ir–N2	177.5 (3)
		N3–Ir–N2	97.2 (3)
		N1–Ir–N2	87.6 (3)
		C7–Ir–N4	168.2 (3)
		C27–Ir–N4	101.4 (3)

Table S3. UV-vis titration data of **1–3** with CT-DNA.

Complexes	Shifts in wavelength (nm)	$\Delta\lambda$ (nm)	Changes in molar extinction coefficient ε ($M^{-1}cm^{-1}$)	$\Delta\varepsilon$($M^{-1}cm^{-1}$)
1	253 – 256	3	8.6×10^4–10.7×10^4	2.1×10^4
2	253 – 255	2	4.5×10^4–7.1×10^4	2.6×10^4
3	252 – 253	1	7.9×10^4–10.0×10^4	2.1×10^4

Table S4. Quenching constant (K_q), binding constant (K_{bin}) and number of binding sites (n) for the interactions of complexes with BSA **1—3**.

Complexes	Temperature (K)	K_q (M^{-1})	K_{bin} (M^{-1})	n	R
1	300	2.84×10^5	2.4×10^6	0.98	0.9964
	310	3.53×10^5	2.6×10^6		0.9967
2	300	2.56×10^5	2.2×10^6	0.95	0.9947
	310	2.93×10^5	2.3×10^6		0.9956
3	300	2.44×10^5	2.1×10^6	0.94	0.9950
	310	2.78×10^5	2.2×10^6		0.9957

Table S5. Log *P* Values for Complexes **1—3**.

Log *P*		
Complex	Mean	SD
1	1.19	0.02
2	1.17	0.03
3	1.13	0.03
Results are the means of three independent experiments and are expressed as means ± SDs.		

Table S6. Most probable binding sites of HSA (PDB ID: 1h9z; Q-site finder) and preferential binding site of the complexes from docked structures.

SITE 1	LYS 195, GLN 196, LEU 198, LYS 199, SER 202, LEU 203, PHE 206, GLY 207, GLU 208, ARG 209, ARG 209, ALA 210, PHE 211, LYS 212, ALA 213, TRP 214, VAL 216, ARG 218, GLN 221, VAL 235, HIS 242, ASN 295 LYS 323, ASP 324, LEU 327, GLY 328, LEU 331, PRO 339, TYR 341, SER 342, VAL 343, VAL 344, LEU 345, LEU 346, LEU 347, ARG 348, ALA 350, LYS 351, GLU 354, GLU 383, Pro 384, LEU 397, ILE 388, LYS 389, ASN 391, CYS 392, PHE 395, PHE 403, LEU 407, ARG 410, TYR 411, LEU 430, GLY 431, Val 433, GLY 434, CYS 437, CYS 438, ARG 445, MET 446, PRO 447, CYS 448, ALA 449, GLU 450, ASP 451, LEU 453, SER 454, VAL 455, LEU 457, VAL 455, LEU 457, ASN 458, SER 480, LEU 481, VAL 482, ARG 484, ARG 485, PRO 486, SER 489
SITE 2	VAL 7, ARG 10, LEU 14, PHE 19, LEU 22, VAL 23, ALA 26, PHE 27, TYR 30, GLU 45, VAL 46, PHE 49 ASN 61, LEU 66, HIS 67, THR 68, LEU 69, PHE 70, ASP 72, LYS 73, THR 76, ASN 99, LRU 103, TYR 150, ALA 151, PRO 152, GLY 248, ASP 249, LEU 250, LEU 251, ALA 254, ASP 255, ARG 257, ALA 258, ALA 261, LEU 283, LEU 284, GLU 285, LYS 286, SER 287, HIS 288
SITE 3	LEU 115, VAL 116, ARG 117, PRO 118, MET 123, PHE 134, LEU 135, TYR 138, LEU 139, ILE 142, HIS 146, PHE 149, LEU 154, PHE 157, ALA 158, TYR 161, LYS 162, PHE 165, LEU 182, ASP 183, LEU 185, ARG 186, GLY 189, LYS 190, SER 193
SITE 4	TYR 401, ASN 405, PHE 502, PHE 507, PHE 509, LYS 524, LYS 525, GLN 526, ALA 528, LEU 529, LEU 532, HIS 535, LYS 536, VAL 547, MET 548, PHE 551, ALA 552, LEU 575, VAL 576, SER 579, GLN 580
SITE 5	GLN 29, LYS 106, ASP 108, HIS 146, PRO 147, TYR 148, PHE 149, TYR 150, ALA 151, GLU 153, SER 192, SER 193, ALA 194, LYS 195, GLN 196, ARG 197, LYS 199, CYS 200, ALA 201, HIS 242, GLU 244, CYS 245, CYS 246, HIS247, GLY 248, ASP 249, LEU 250, CYS 253, ARG 257
1	LYS 205, PHE 206, ARG 209, ALA 210, ALA 213, LEU 347, ARG 348, LYS 351, GLU 354, THR 478, GLU 479, SER 480, LEU 481, VAL 482.
2	GLU 153, SER 192, LYS 195, GLN 196, LYS 199, SER 202, PHE 211, TRP 214, ARG 218, ARG 222, HIS 242, ARG 257, SER 287, HIS 288, ALA 291, GLU 292, ASP 451, SER 454, LEU 481.
3	LYS 195, ARG 218, ARG 222, LYS 274, ALA 291, GLU 292, GLU 294, ASN 295, PRO 339, ASP 340, HIS 440, ALA 443, LYS 444, PRO 447, CYS 448, ASP 451.